

Supporting Information

Sub-mm³ Dimensional Scaling of Fully-Integrated Additively-Fabricated Microsupercapacitors for Embedded Energy Storage Applications

Amin Hodaie¹, Vivek Subramanian^{1,2}*

¹Laboratory for Advanced Fabrication Technologies, Institute of Electrical and Microengineering, École polytechnique fédérale de Lausanne (EPFL), Neuchâtel 2002, Switzerland

²Department of Electrical Engineering and Computer Sciences, University of California, Berkeley, CA, 94720-1770, USA

Corresponding author: vivek.subramanian@epfl.ch

Keywords: microsupercapacitors, dimensional Scaling, 3D printing, additive fabrication, energy storage, edge-oxidized graphite oxide (EOGO), cerium oxide

Table S1. The IDs of the 3D printed microsupercapacitors and their related geometrical feature dimensions

MSC ID	Width of the fingers (W) (mm)	Length of the fingers (L) (mm)	Gap between the fingers (G) (mm)	Active Area's Lateral dimensions ((2W+G) × L) (mm × mm)	Active area (cm ²)*
XS1	0.35	2.5	0.75	1.45 × 2.5	0.04375
XS2	0.35	3.75	0.75	1.45 × 3.75	0.065625
XS3	0.35	5	0.75	1.45 × 5	0.0875
S1	0.5	2.5	0.75	1.75 × 2.5	0.04375
S2	0.5	3.75	0.75	1.75 × 3.75	0.065625
S3	0.5	5	0.75	1.75 × 5	0.0875
M1	0.75	2.5	0.75	2.25 × 2.5	0.05625
M2	0.75	3.75	0.75	2.25 × 3.75	0.084375
M3	0.75	5	0.75	2.25 × 5	0.1125
L1	1	2.5	0.75	2.75 × 2.5	0.06875
L2	1	3.75	0.75	2.75 × 3.75	0.103125
L3	1	5	0.75	2.75 × 5	0.1375

*calculations of the active area is based on the rectangular area (i.e., the dashed yellow rectangles as shown in Figures S1-S12) surrounding the current collector fingers which is theoretically the maximum area that the electrodes can take up after printing.

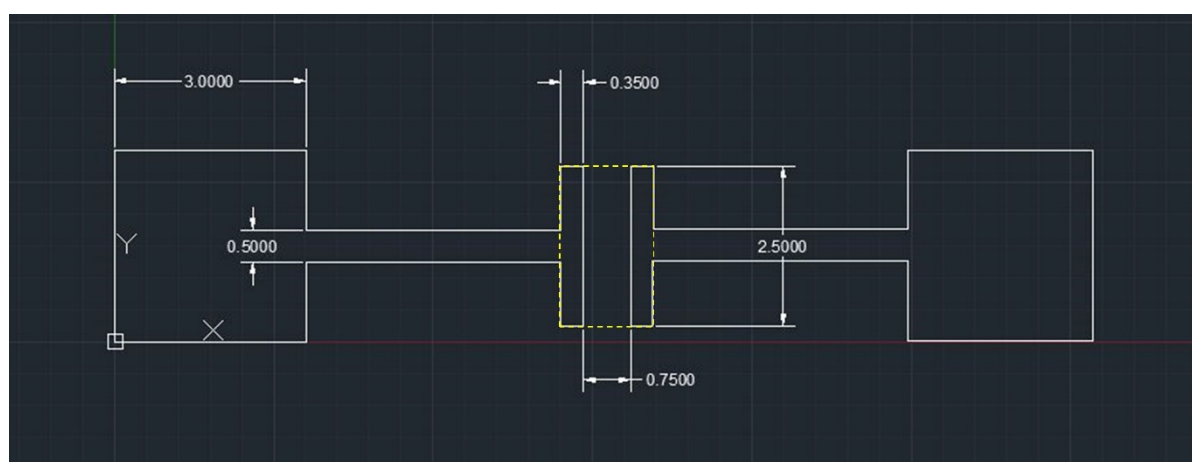


Figure S1. The geometrical details of the design of the current collectors of the MSC with the sample ID XS1.

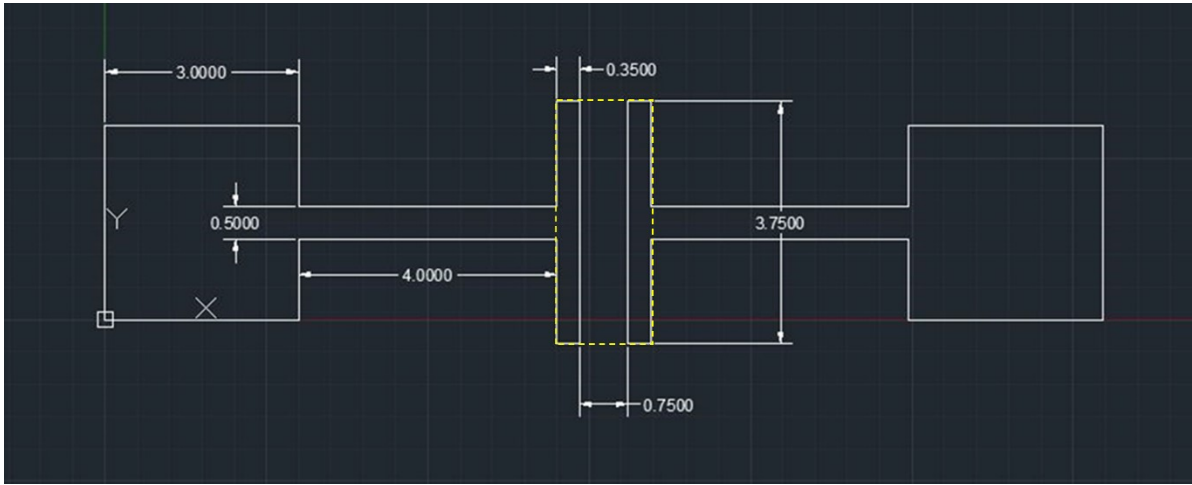


Figure S2. The geometrical details of the design of the current collectors of the MSC with the sample ID XS2.

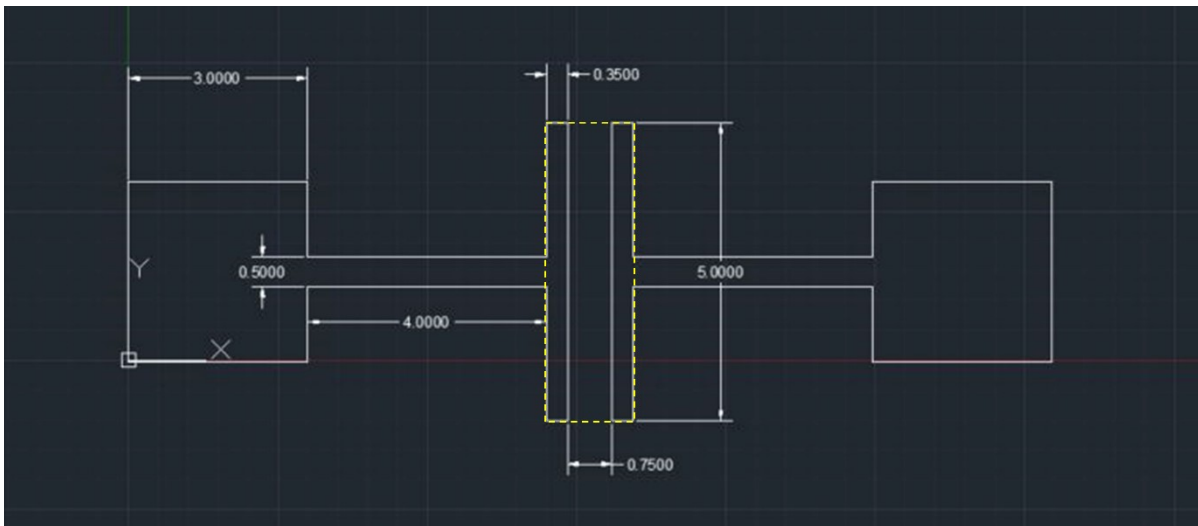


Figure S3. The geometrical details of the design of the current collectors of the MSC with the sample ID XS3.

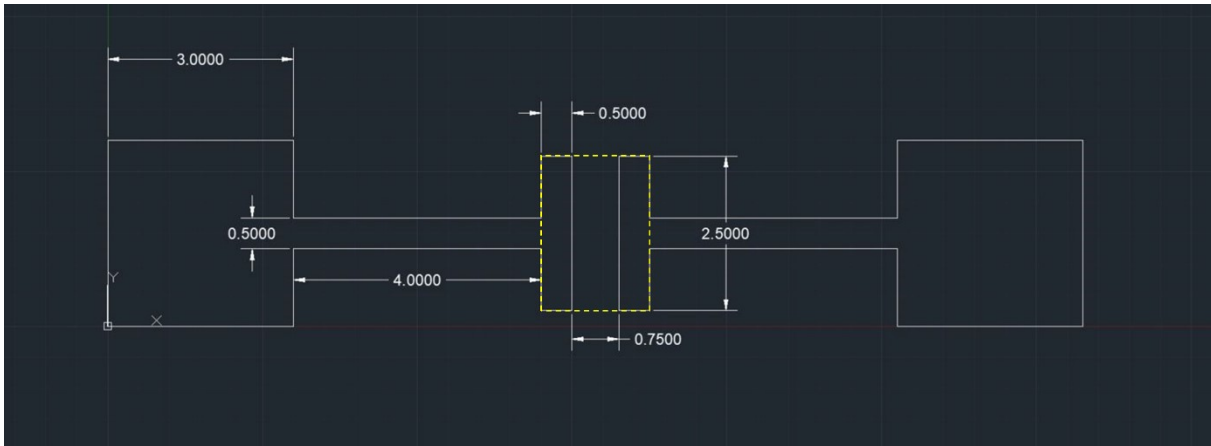


Figure S4. The geometrical details of the design of the current collectors of the MSC with the sample ID S1.

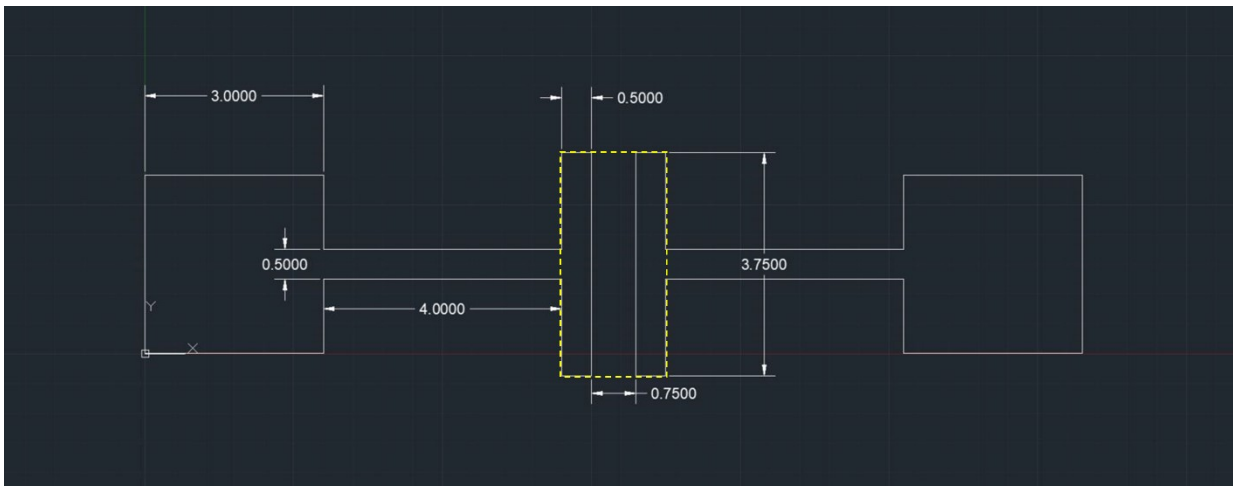


Figure S5. The geometrical details of the design of the current collectors of the MSC with the sample ID S2.

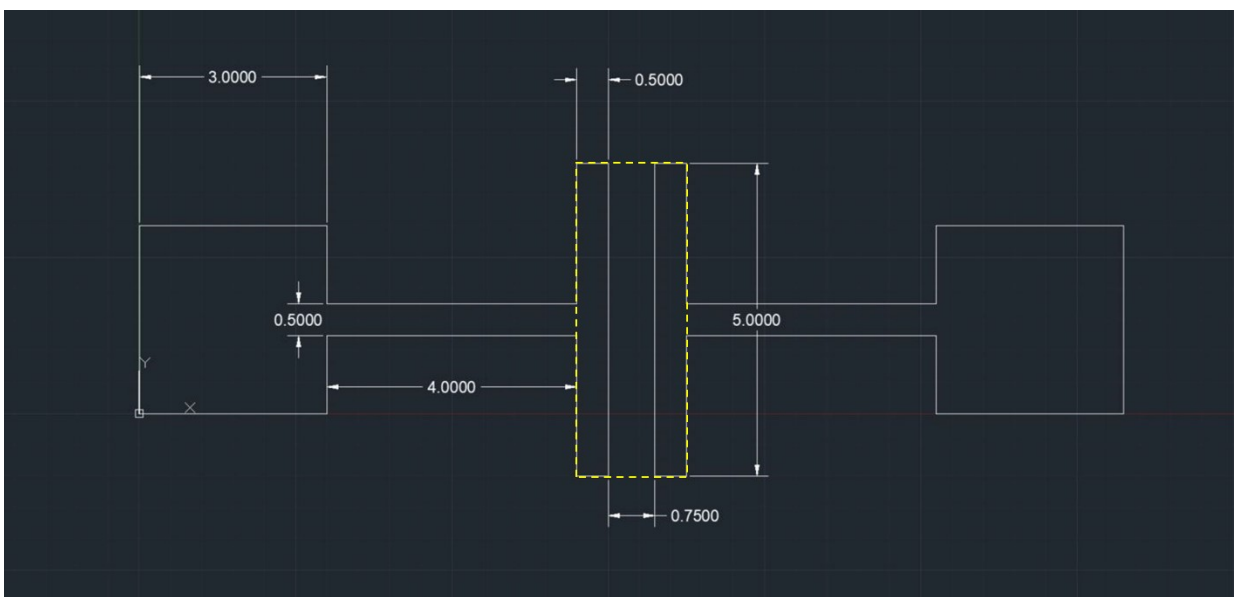


Figure S6. The geometrical details of the design of the current collectors of the MSC with the sample ID S3.

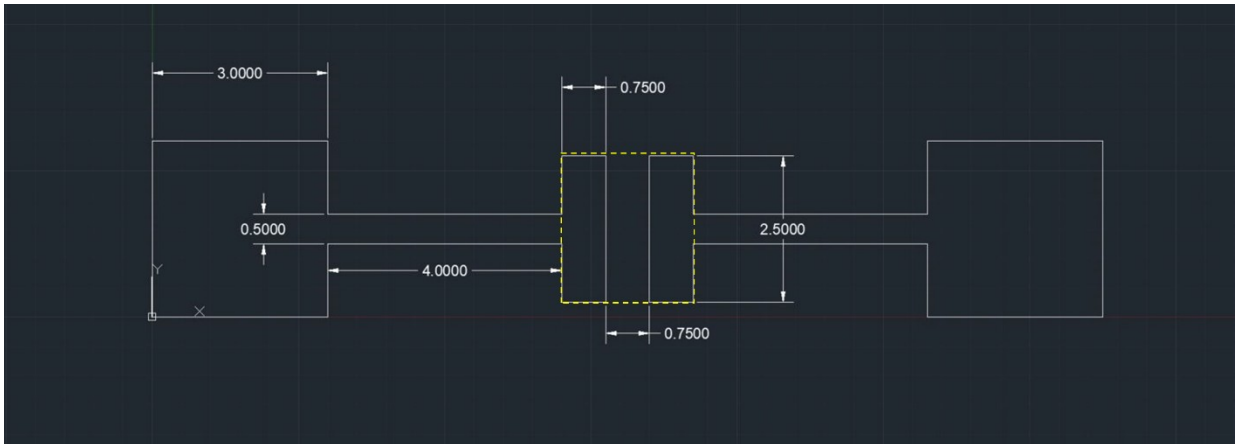


Figure S7. The geometrical details of the design of the current collectors of the MSC with the sample ID M1.

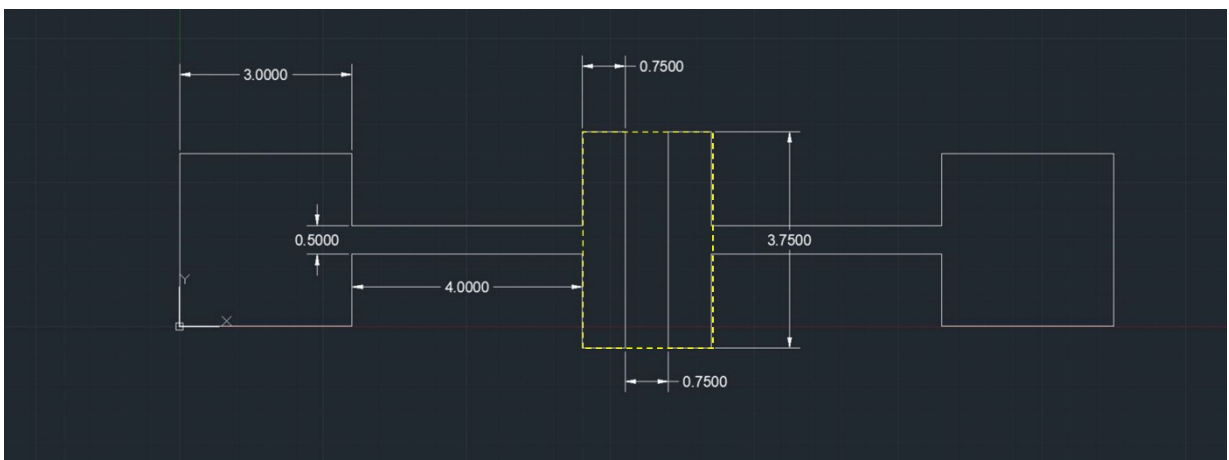


Figure S8. The geometrical details of the design of the current collectors of the MSC with the sample ID M2.

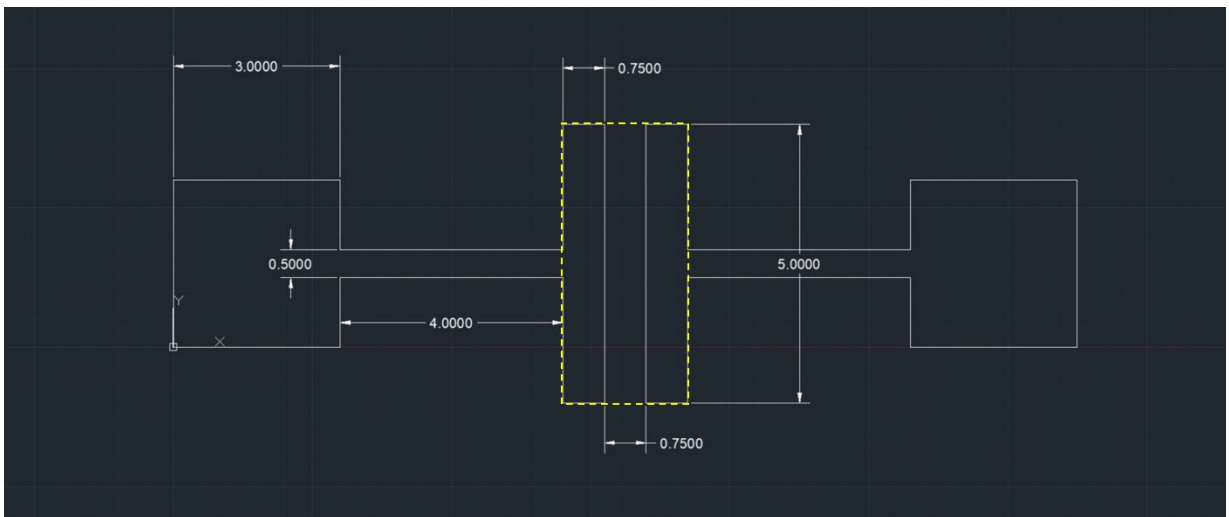


Figure S9. The geometrical details of the design of the current collectors of the MSC with the sample ID M3.

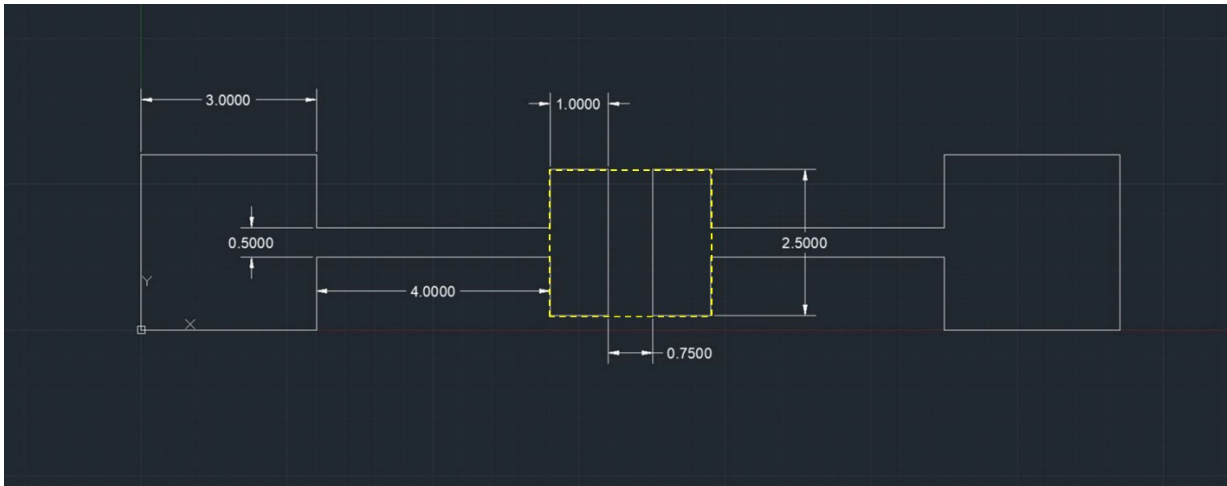


Figure S10. The geometrical details of the design of the current collectors of the MSC with the sample ID L1.

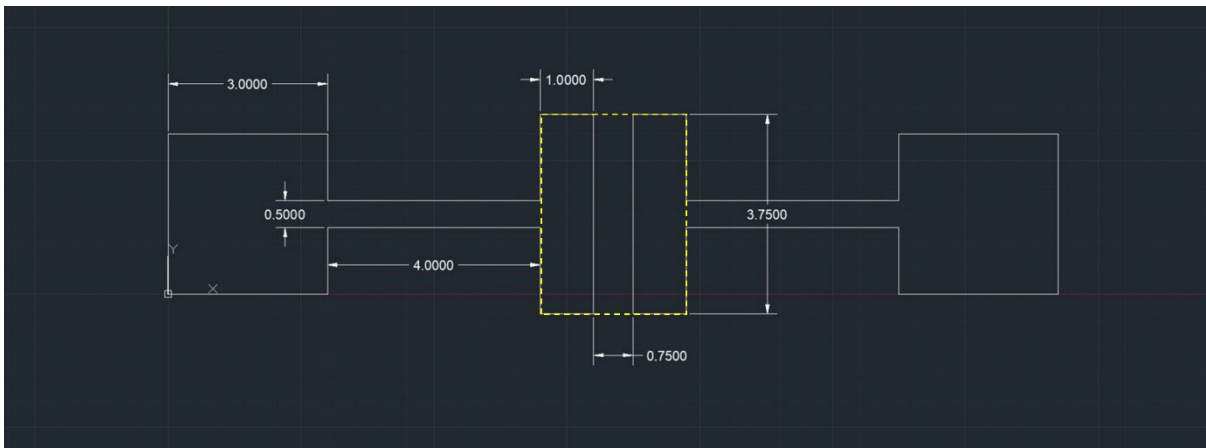


Figure S11. The geometrical details of the design of the current collectors of the MSC with the sample ID L2.

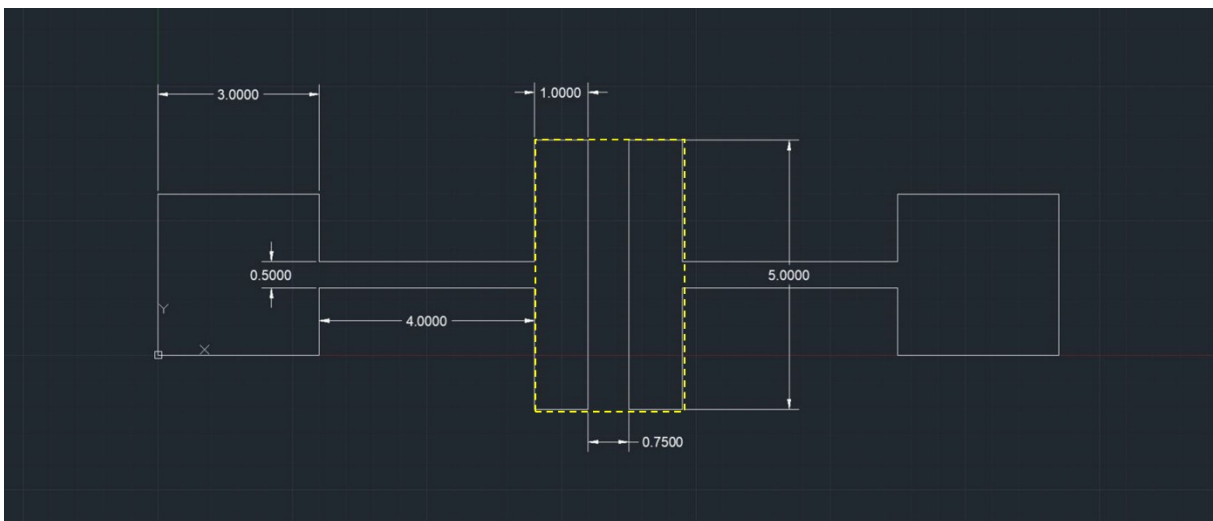


Figure S12. The geometrical details of the design of the current collectors of the MSC with the sample ID L3.

Electrochemical performance calculations

The areal and volumetric capacitances, the energy density and the power density of the fully 3D printed MSCs were calculated based on the equations below using the CV curves^[1]:

$$C_A = \frac{\int_0^{0.6} j dV}{A \times \Delta V \times v}$$

(S1)

$$C_{Vol} = \frac{C_A}{h}$$

(S2)

$$E_A = \frac{C_A \times V^2}{2 \times 3.6}$$

(S3)

$$P_A = \frac{E_A \times v \times 3600}{\Delta V}$$

(S4)

Where C_A (mF/cm²) is the areal capacitance of the device, A (cm²) is the active area of the MSC, E_A is the areal energy density (μWh/cm²), P_A is the areal power density (μW/cm²), j is the current (mA), ΔV is the voltage window (0.6 V), h is the height of the electrodes, and v is the scan rate (mV/s).

We also used GCD curves to calculate the areal and volumetric capacitances of the MSCs using the equations below^[2]:

$$C_{A(GCD)} = \frac{I \times \Delta t}{A \times \Delta V}$$

(S5)

$$C_{Vol(GCD)} = \frac{C_A}{h}$$

(S6)

Where $C_{A(\text{GCD})}$ (mF/cm²) is the areal capacitance of the device, A (cm²) is the active area of the MSC, Δt is discharging time, h is the height of the electrodes and ΔV is potential change during the discharge.

Kinetic study of charge storage mechanisms

We calculated the ratio of (EDLC + Faradaic pseudocapacitance) (fast kinetic)/diffusive ion insertion (diffusive pseudocapacitance) (slow kinetic) charge storage contributions of the MSCs comprising 3.75 mm electrodes printed with the smallest nozzle (i.e., 250 μm) and the largest nozzle (i.e., 840 μm) as a function of the sweep rates (ν) using the CV measurements according to a method introduced by Trasatti.^[3] These calculations differentiate the fast-kinetic charge storage (EDLC + Faradaic pseudocapacitance—outer surface) and the slow-kinetic charge storage (diffusive ion insertion—diffusive pseudocapacitance—inner surface) mechanisms. The value of the fast-kinetic (outer surface) areal capacitance $(C_A)_o$ is obtained from the extrapolation of areal capacitance (C_A) to $\nu=\infty$ derived from the plot of areal capacitance (C_A) vs. $\nu^{-0.5}$. And, the value of the total areal capacitance $(C_A)_t$ is obtained from the extrapolation of inverse of areal capacitance $(C_A)^{-1}$ to $\nu=0$ from the plot of inverse of areal capacitance $(C_A)^{-1}$ vs. $\nu^{0.5}$. By calculating the C_o and C_t , one can calculate the C_i (inner surface capacitance—diffusive ion insertion—diffusive pseudocapacitance) using equation S4.

$$(C_A)_t = (C_A)_i + (C_A)_o \quad (\text{S4})$$

Where $(C_A)_t$ is the total areal capacitance (mF.cm⁻²), $(C_A)_i$ is the inner surface areal capacitance stemming from the slow-kinetic charge storage (diffusive ion insertion—diffusive pseudocapacitance—inner surface) (mF.cm⁻²), and $(C_A)_o$ is the outer surface areal capacitance caused by the fast-kinetic charge storage (EDLC + Faradaic pseudocapacitance—outer surface) (mF.cm⁻²). We used the intercepts of the Y axes in these plots using the values shown in their legends to calculate $(C_A)^{-1}$ and (C_A) .

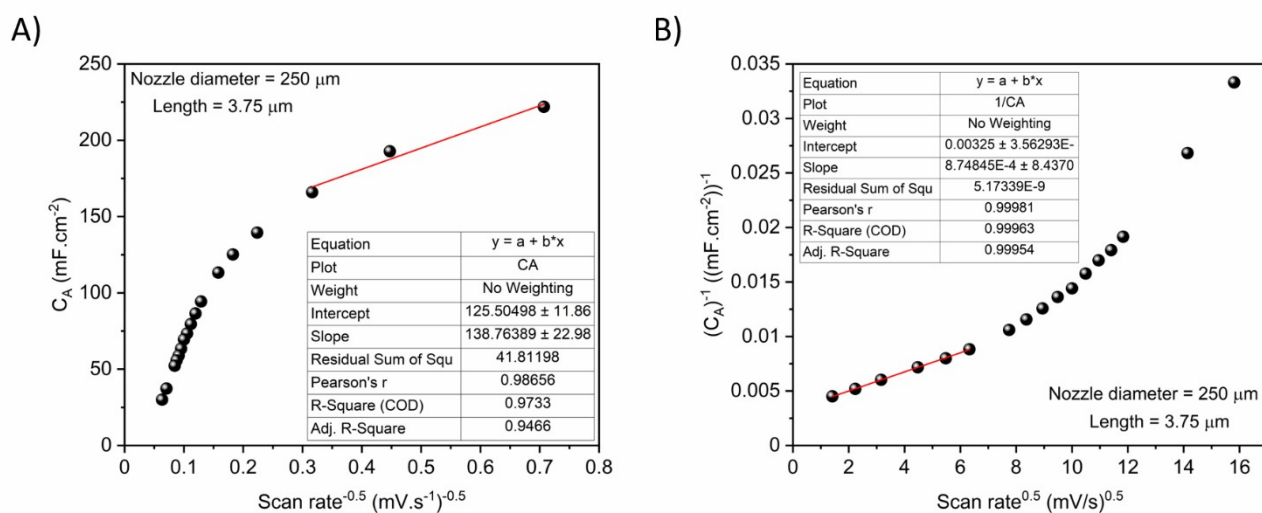


Figure S13. The plots of A) C_A vs. $u^{-0.5}$ and B) C_A^{-1} vs. $u^{0.5}$ of the MSC constructed by the electrode with the length of 3.75 mm, which is printed with a nozzle of diameter 250 μm.

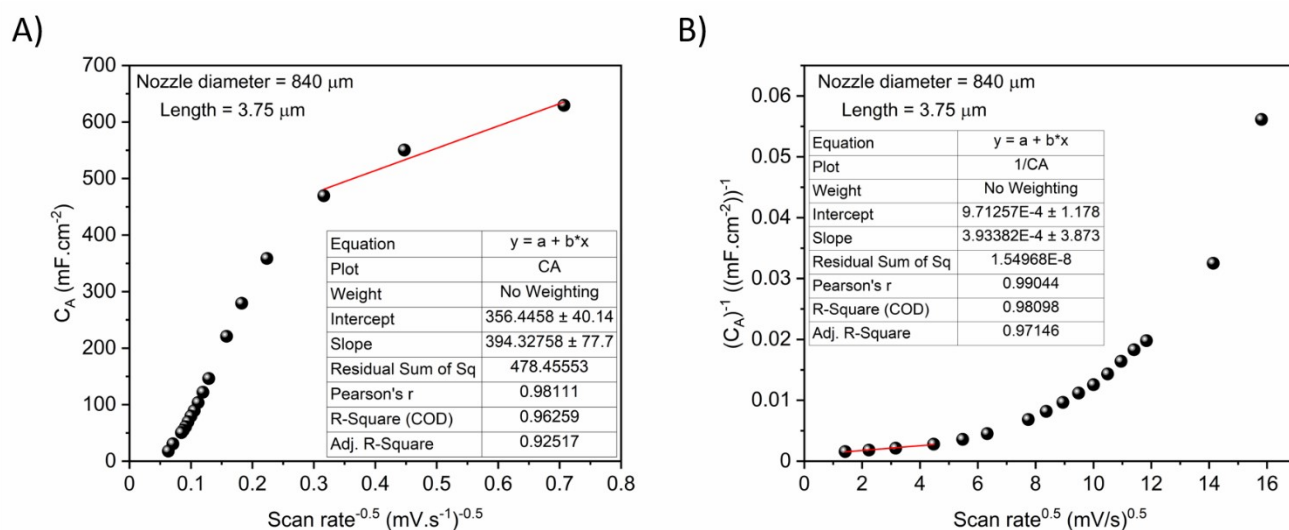


Figure S14. The plots of A) C_A vs. $u^{-0.5}$ and B) C_A^{-1} vs. $u^{0.5}$ of the MSC constructed by the electrode with the length of 3.75 mm, which is printed with a nozzle of diameter 840 μm.

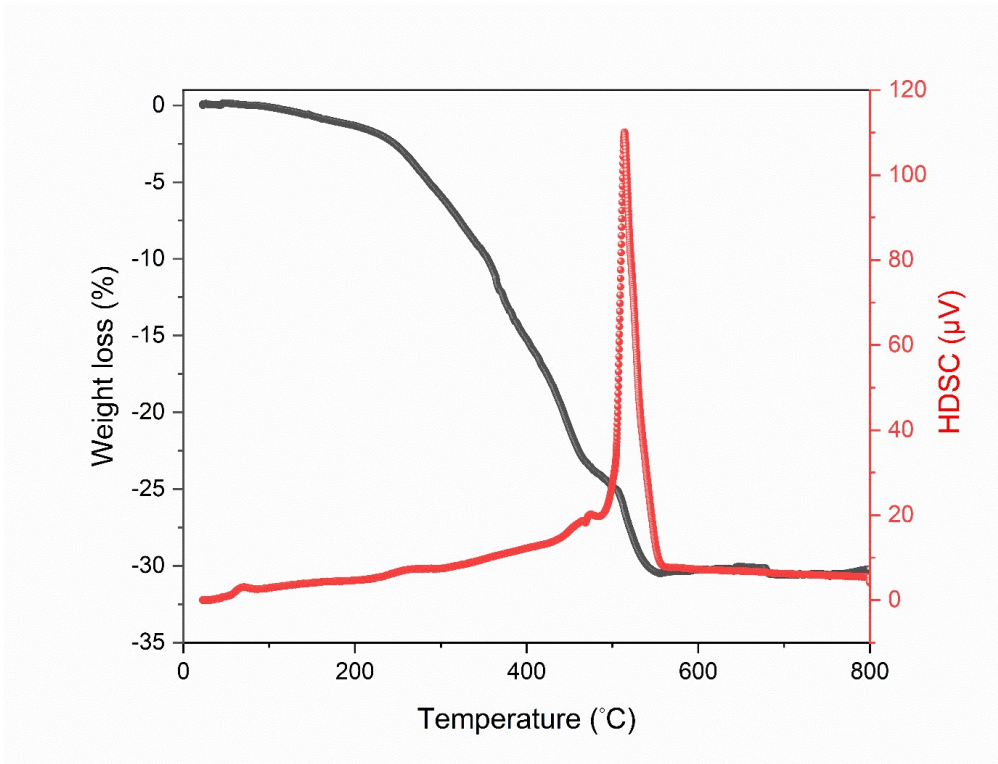


Figure S15. TGA and DSC curves of the silver paste used for 3D printing of the current collector.

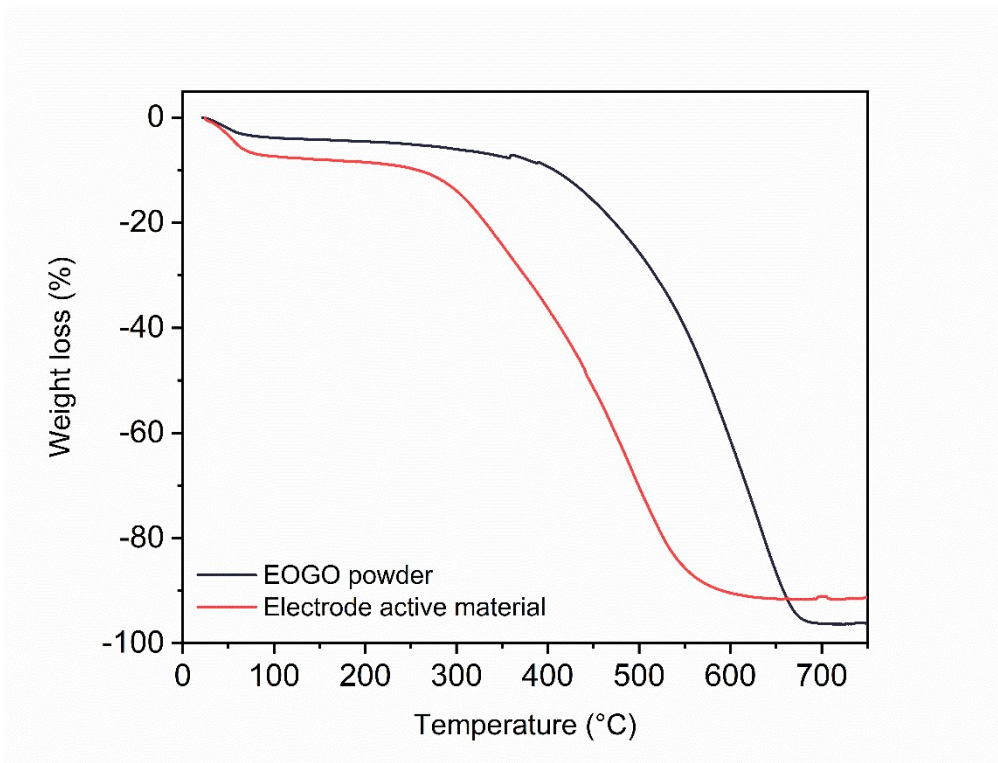


Figure S16. Thermogravimetric analysis (TGA) plots of all the electrode active materials.

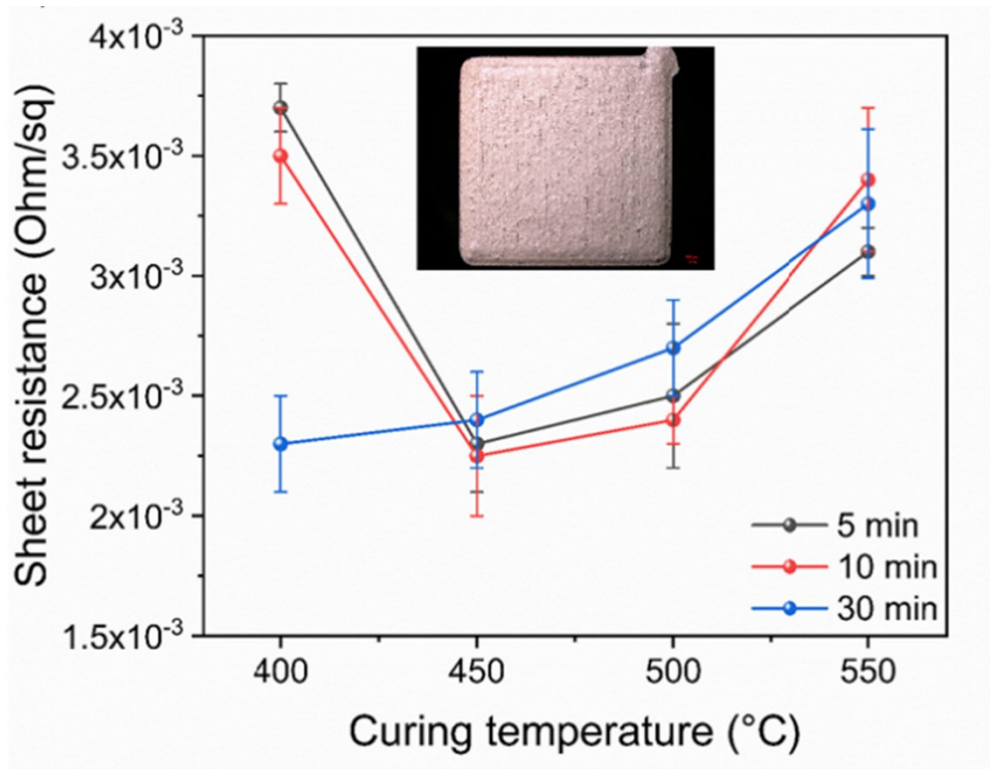


Figure S17. Sheet resistance of the silver paste used for the current collector fabrication as a function of heat treatment temperature and duration in air.

We also performed XPS spectroscopy to elucidate the presence of different oxidation states of cerium (i.e., Ce(III) and Ce(IV)) in the electrode active material.

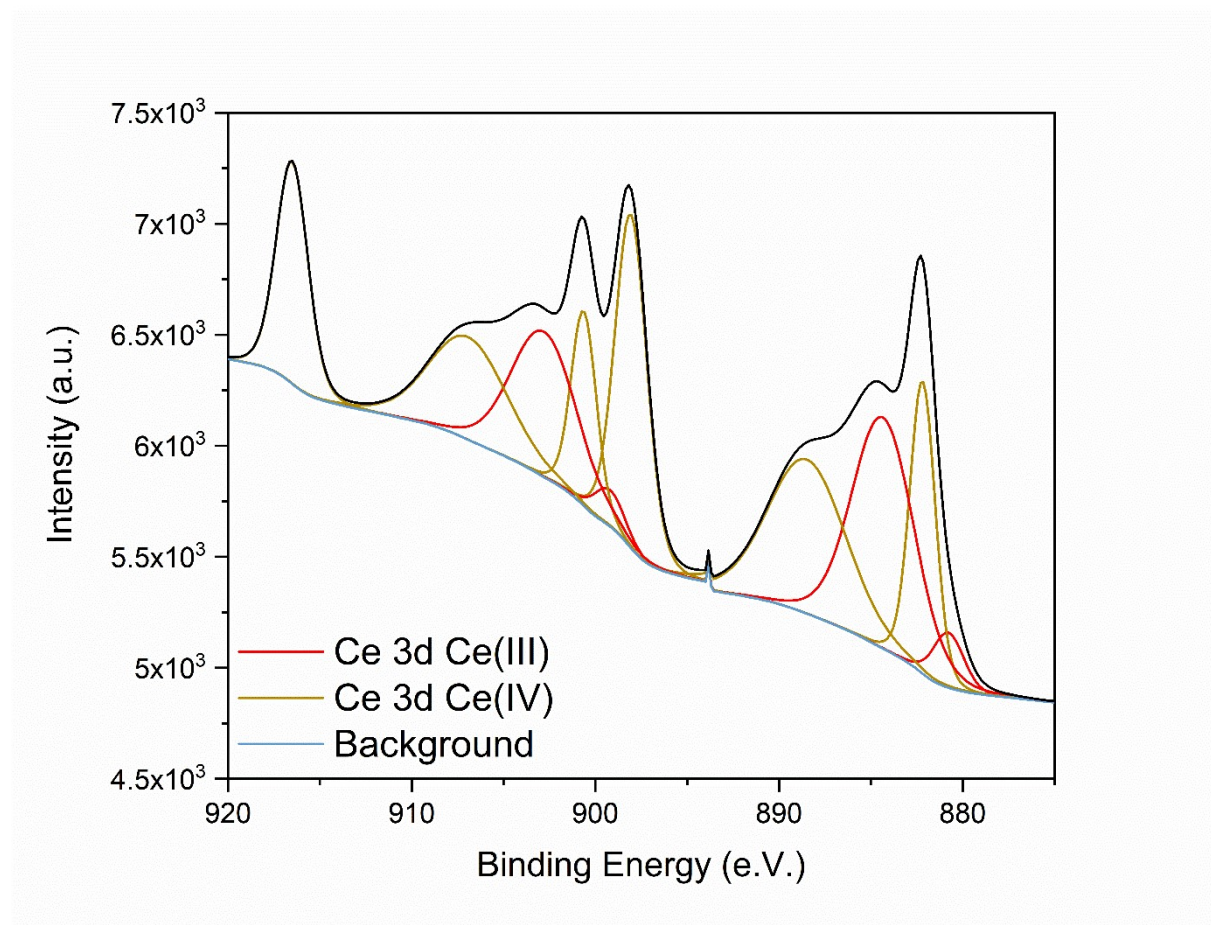


Fig. S18. Deconvoluted Ce 3d region of XPS spectrum of the electrode active material.

Table S2. Assignment of Ce oxidation state associated with deconvoluted peaks in the Ce 3d region of XPS spectrum of the electrode active material.

Deconvoluted peak binding energy (e.V.)	Oxidation state of Ce associated with the deconvoluted peak
880.45-880.77	Ce(III)
882.28-882.3	Ce(IV)
884.24-885.1	Ce(III)
888.29-888.58	Ce(IV)
898.05-898.9	Ce(IV)
898.9-899.22	Ce(III)
900.73-900.75	Ce(IV)
902.69-903.55	Ce(III)
906.74-907.03	Ce(IV)
916.5-916.62	Ce(IV)

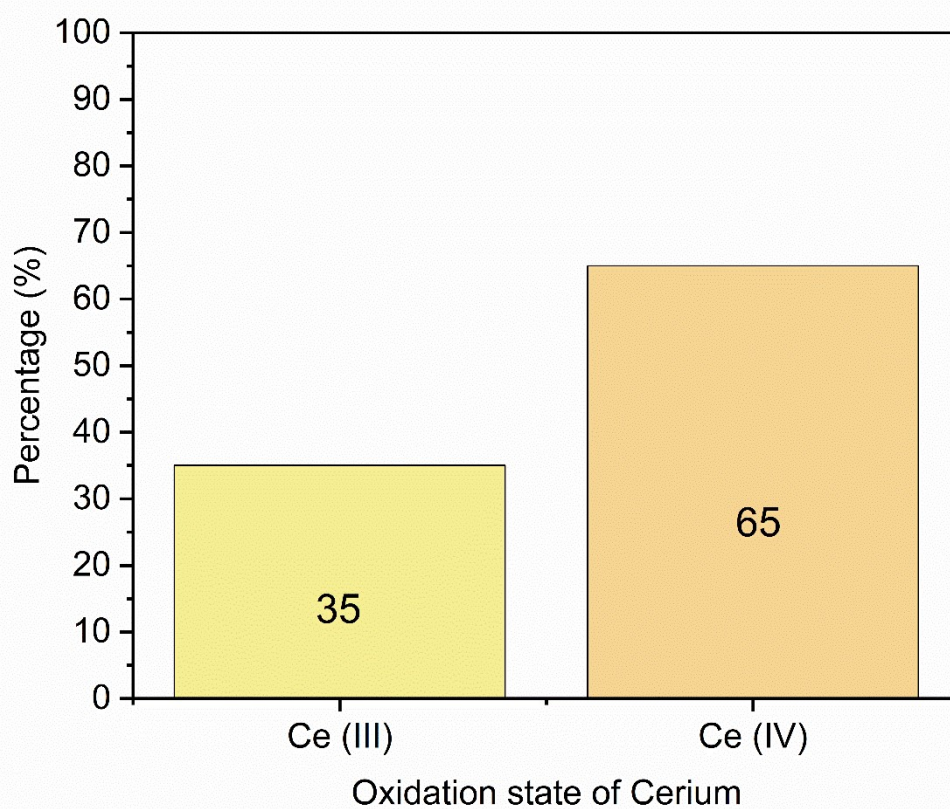


Figure S19. Oxidation states of Cerium in the electrode active material that is a nanocomposite of EOGO (~95 wt.%) / cerium oxide NPs (~5 wt.%).

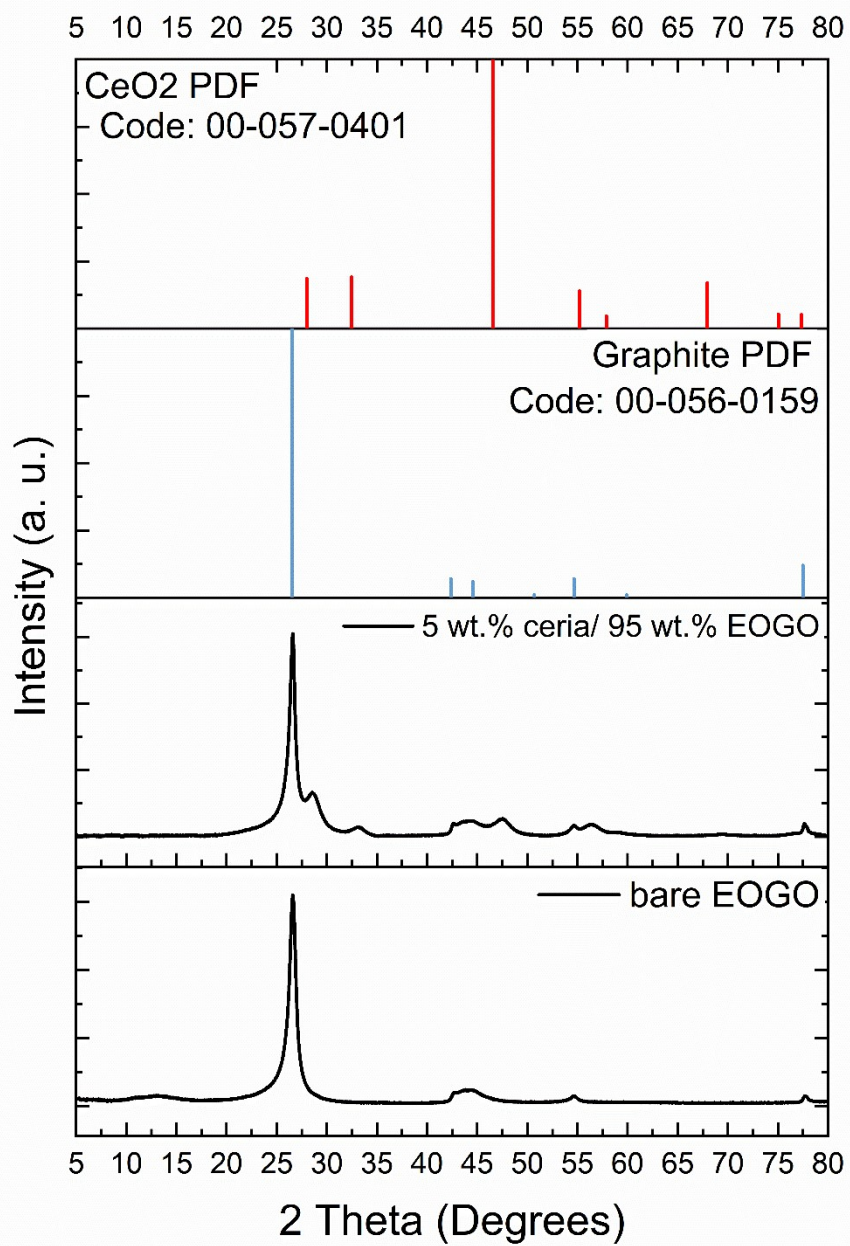


Figure S20. XRD plots of the bare EOGO powder and the electrode active material (i.e., nanocomposite based on EOGO (95 wt.%)/cerium oxide NPs (5 wt.%) nanocomposites and PDF files of graphite and CeO₂ showing their corresponding characteristic peaks.

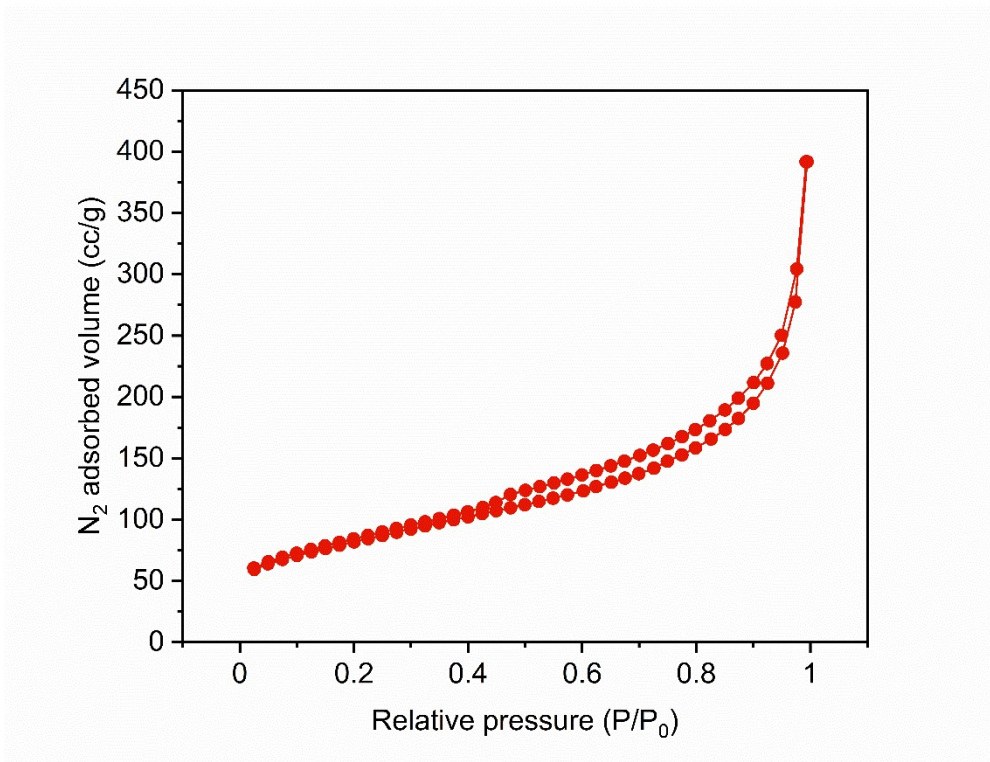


Figure S21. N₂ adsorption isotherm of the electrode active material.

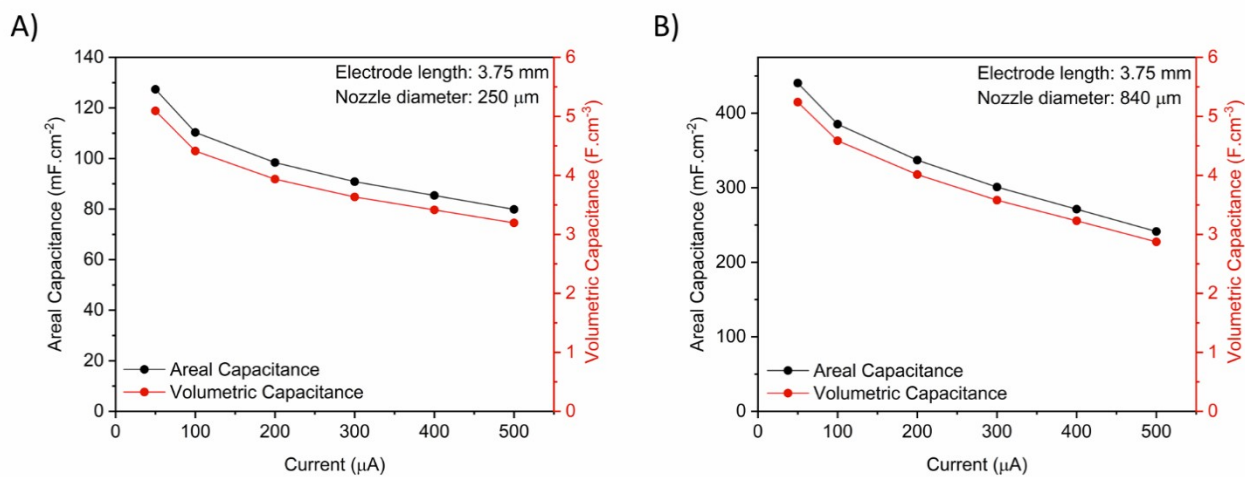


Figure S22. Areal and volumetric capacitances as a function of current using the GCD measurements of the MSCS (IDs: XS2 and L2) with a nozzle diameter of A) 250 μm , and B) 840 μm .

We also performed EIS measurements to extract the equivalent circuit of the MSC cycled for 17000 cycles and its corresponding values, i.e., R_s is the ESR, ($R_s - R_p = R_{ct}$ (i.e., charge transfer resistance)).

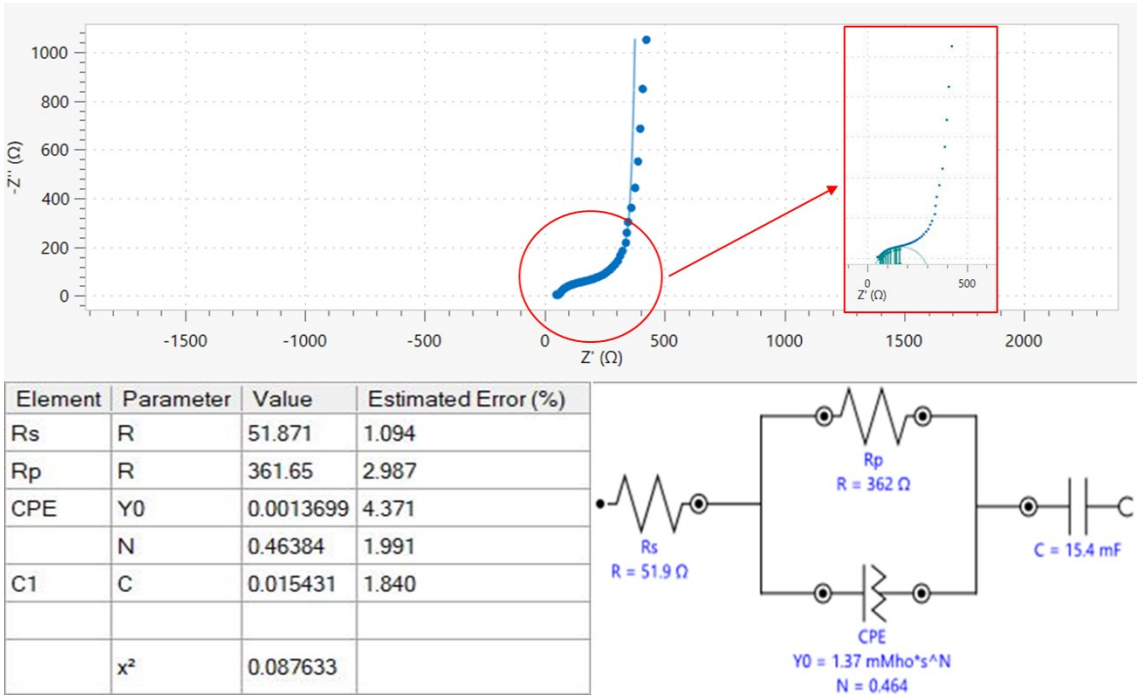


Figure S23. EIS plot, equivalent circuit, and corresponding values of this circuit of an MSC comprising an electrode of 3.75 mm long electrode printed with the nozzle of 840 μm .

References

- [1] S. Abdolhosseinzadeh, R. Schneider, A. Verma, J. Heier, F. Nüesch, C. (John) Zhang, *Adv. Mater.* **2020**, *32*, 2000716.
- [2] S. Sollami Delekta, K. H. Adolfsson, N. Benyahia Erdal, M. Hakkarainen, M. Östling, J. Li, *Nanoscale* **2019**, *11*, 10172.
- [3] S. Ardizzone, G. Fregonara, S. Trasatti, *Electrochimica Acta* **1990**, *35*, 263.